

Chapter

**7**

## **Atmospheres**

Atmospheres are found on the Sun, eight of the nine planets, and three of the sixty-one satellites, for a total count of a dozen. Each has its own brand of weather and its own unique chemistry. In this chapter we will compare and contrast their vertical structure and chemistry, and in the next chapter we will investigate the fluid dynamics that governs their weather and climate patterns.

Atmospheres can be divided into two major groups: the terrestrial-planet atmospheres, which have solid surfaces (or oceans) as their lower boundary condition, and the gas-giant atmospheres, which are essentially bottomless. Venus and Titan form one terrestrial-planet subgroup that is characterized by slowly rotating surfaces and rapidly rotating atmospheres. Mars, Io, Triton, and Pluto form a different subgroup that is characterized by thin atmospheres that are in large measure driven by vapor-pressure equilibrium with frozen volatiles on their surfaces. Both Io and Triton have active volcanic plumes that influence their atmospheres. Earth's atmosphere is affected by mountain ranges that frustrate the tendency for winds to settle into steady east-west patterns. In addition, Earth's atmospheric eddies are comparable in size to the planet itself, which is also true of Mars but is unlike any other atmosphere. For Earth, this cramped environment contributes to the most unpredictable weather in the solar system.

The gas-giant atmospheres include the four giant planets and the Sun, which together

constitute five variations on a single theme of a rotating ball of hydrogen and helium gas. Jupiter and Saturn form one gas-giant subgroup that is characterized by eastward-moving equatorial winds and a dozen midlatitude jet streams. Uranus and Neptune form a subgroup that is characterized by westward-moving equatorial winds and one broad, midlatitude jet per hemisphere. Jupiter has hundreds of long-lived oval-shaped storms, the largest being the Great Red Spot, whereas Saturn has dozens of storms and Neptune has just two. One of Neptune's storms, the Great Dark Spot, is remarkably similar to Jupiter's Great Red Spot. Uranus stands out as the only giant planet that does not have oval-shaped storms, the only one tipped on its side, and the only one without a significant internal heat source.

## 7.1 The Basics

### 7.1.1 Hydrostatic Equilibrium

As an initial step towards understanding the basics of atmospheric structure, consider the case of **hydrostatic equilibrium** in which an atmosphere is gravitationally bound to a planet. The atmospheric pressure,  $p$  takes the form

$$p(r) = \int_r^\infty \rho(r) g(r) dr \quad (7.1)$$

where  $r$  is radial distance from the center of the planet,  $\rho = m_r n$  is mass density, where  $m_r$  is the average mass per gas molecule,  $n$  is the number density of molecules, and

$$g = \frac{GM}{r^2},$$

where  $G$  is the Universal constant of gravitation and  $M$  is the planetary mass. Integrating (7.1) we see that

$$\frac{dp}{dr} = -\rho g, \quad (7.2)$$

where the minus sign indicates that gravity increases inward. Equation (7.2) is called the **hydrostatic equation**. For a thin atmosphere in which  $\Delta r \ll r$ ,  $g(r)$  can be treated as a constant and

$$g \approx \frac{GM}{a^2}, \quad (7.3)$$

where  $a$  is the radius of the solid planet.

### 7.1.2 Equation of State

To derive a simple equation of state for an atmosphere we invoke the ideal gas law

$$pV = NkT \quad (7.4)$$

where  $V$  is volume,  $T$  is temperature,  $N$  is the total number of gas molecules, and  $k$  is Boltzmann's constant that is related to the gas constant  $R$  by

$$R = \frac{k}{m_r} = k \frac{N_o}{M_r}, \quad (7.5)$$

where  $M_r$  is the average molecular mass per mole, and  $N_o = 6.023 \times 10^{23} \text{ mol}^{-1}$  is Avogadro's number. Substituting (7.5) into (7.4) it is apparent that

$$p = \rho RT. \quad (7.6)$$

Expression (7.6) is the simplest and most commonly used equation of state in atmospheric science.

Although  $R$  is known as the gas constant it has different values for different planets. From (7.6) we can estimate  $R$  for Earth's atmosphere. Given  $M_r = 0.029 \text{ kg mole}^{-1}$  we find that  $R = 287 \text{ J kg}^{-1} \text{ K}^{-1}$ .

### 7.1.3 Atmospheric Scale Height

We may next combine (7.2) and (7.6) to get

$$\frac{dp}{dr} = -\frac{gp}{RT}.$$

We re-arrange to get

$$\frac{dp}{p} = -\frac{g}{RT} dr,$$

which may be integrated to get

$$p(r) = p(r_o) \exp \left[ \int_{r_o}^r -\frac{g}{RT} dr \right].$$

We now consider the special case of an **isothermal atmosphere**, in which the temperature is the same at all altitudes. For an isothermal atmosphere we define a constant temperature  $T = T_o$  where

$$\frac{1}{H} \equiv \frac{g}{RT} = \frac{g}{RT_o} \quad (7.7)$$

where  $H$  is the **atmospheric scale height** that describes to first order the vertical structure of the atmosphere. Then

$$p(r) = p(r_o) \exp \left[ \frac{r_o - r}{H} \right]. \quad (7.8)$$

From (7.8) we see that in an isothermal atmosphere pressure falls off exponentially with height. From (7.6) we may also conclude that density falls off exponentially with height. The physical interpretation of the scale height is that it represents the change in height

over which pressure or density falls off by a factor of  $1/e$  ( $\approx 1/2.7$ ). For the terrestrial planets with atmospheres the scale heights are about 10 km. In practice, temperature changes with altitude and so atmospheric structure is more complex than a simple exponential. We return to this point later.

## 7.2 Radiative Transfer

### 7.2.1 Effective Temperature

In Chapter 4 we defined the effective temperature ( $T_e$ ) of an object to be the temperature of a blackbody that has the same radiative flux  $\sigma T_e^4$  as the object. We can obtain an expression for  $T_e$  by considering the case of **thermal equilibrium** where the absorbed and emitted radiation on the planet are balanced. The absorbed radiation  $B$  will have the form

$$B = \pi a^2(1 - A) \frac{s}{R_p^2} \quad (7.9)$$

where  $A$  is albedo,  $s = 1370 \text{ W m}^{-2}$  is the solar constant, *i.e.* the solar flux at 1 AU, and  $R_p$  is the distance from the planet to the sun in AU. For the emitted radiation  $B_\nu(T)$  we assume a black body and recall from Chapter 4

$$B_\nu(T) = \frac{2h\nu^3}{c^2} \frac{1}{e^{\frac{h\nu}{kT}} - 1}$$

and integrate over frequency  $\nu$

$$B(T) = \int_0^\infty B_\nu(T) d\nu = \int_0^\infty \frac{d\nu}{e^{\frac{h\nu}{kT}} - 1}$$

which yields

$$B(T) = \sigma T^4 \quad (7.10)$$

which is the **Stefan-Boltzmann Law**, in which  $\sigma$

$$\sigma = \frac{2\pi^5}{15} \frac{k^4}{h^3 c^2}.$$

is the Stefan-Boltzmann constant. Next, the radiative flux ( $F$ ) from a surface ( $\Omega$ ) can be expressed

$$F = \int_{2\Omega} B \cos\theta d\Omega = 2\pi \int_0^{\frac{\pi}{2}} B \cos^2\theta d\theta = \pi B,$$

where  $\theta$  is the angle from the vertical. A full expression for the radiative flux is

$$\pi B(T) = \sigma T^4$$

and the total radiation emitted from the planet is

$$4\pi a^2 F = 4\pi a^2 \sigma T_e^4. \quad (7.11)$$

For radiative equilibrium we equate (7.9) and (7.11)

$$\pi a^2(1 - A) \frac{s}{R_p^2} = 4\pi a^2 \sigma T_e^4$$

which yields the effective temperature

$$T_e = \left[ \frac{(1 - A) s}{4\sigma R_p^2} \right]^{\frac{1}{4}}. \quad (7.12)$$

From (7.12) the effective temperatures of Venus, Earth, and Mars are about 500, 33, and 5 K *lower* than their surface temperatures, respectively. This disparity is caused by the **greenhouse effect**, which arises when an atmosphere is more transparent to incoming radiation than to outgoing radiation.

### 7.2.2 The Greenhouse Effect

As a simple model of the greenhouse effect, consider a thin layer of gas with a vertical thickness  $\Delta z$ , constant density  $\rho$ , and temperature  $T_{\text{gas}}$  that hovers above a flat surface with a temperature  $T_{\text{sur}}$ . We will assume the gas is transparent to the incoming visible flux from the Sun,  $F_{\text{solar}}$ , but partially absorbs the outgoing infrared flux from the surface,  $\sigma T_{\text{sur}}^4$ . For an absorbing medium, we define the ratio of transmitted flux to incident flux at wavelength  $\lambda$  to be:

$$\frac{\text{transmitted flux}}{\text{incident flux}} \equiv e^{-\tau(\lambda)}, \quad (7.13)$$

where  $\tau(\lambda)$  is called the **optical depth** of the absorbing medium. The exponential function in (7.13) is used here for its property of converting multiplications into additions of exponents, such that the total optical depth of a series of absorbing layers is just the sum of the optical depths of the individual layers. For a continuously varying absorber the optical depth at a particular wavelength is expressed in terms of the path integral of the density  $\rho(z)$  and the **absorption coefficient**  $k(z, \lambda)$ :

$$\tau(z, \lambda) = \int_z^\infty \rho(z') k(z', \lambda) dz'. \quad (7.14)$$

For now we will assume  $k(\text{visible}) = 0$  and  $k(\text{infrared}) = k$  for our thin layer of gas, such that:

$$\tau(\text{visible}) = 0, \quad \tau(\text{infrared}) = \rho k \Delta z.$$

The gas absorbs some of the infrared radiation coming up from below and then radiates in both the upward and downward directions. Thermal equilibrium is reached when the upward and downward fluxes are equal. The flux balance above the layer of gas is

$$\uparrow (\sigma T_{\text{gas}}^4 + \sigma T_{\text{sur}}^4 e^{-\tau}) = \downarrow (F_{\text{solar}}), \quad (7.15)$$

and the flux balance below the layer of gas is:

$$\uparrow (\sigma T_{\text{sur}}^4) = \downarrow (F_{\text{solar}} + \sigma T_{\text{gas}}^4) . \quad (7.16)$$

Together these can be expressed in matrix form:

$$\begin{pmatrix} 1 & e^{-\tau} \\ -1 & 1 \end{pmatrix} \begin{pmatrix} T_{\text{gas}}^4 \\ T_{\text{sur}}^4 \end{pmatrix} = \frac{F_{\text{solar}}}{\sigma} \begin{pmatrix} 1 \\ 1 \end{pmatrix} . \quad (7.17)$$

For problems with more than one absorbing layer a larger matrix results. Using the fact that the inverse of a two-by-two matrix is:

$$\begin{pmatrix} a & b \\ c & d \end{pmatrix}^{-1} = \frac{1}{ad - bc} \begin{pmatrix} d & -b \\ -c & a \end{pmatrix} ,$$

the temperatures work out to be:

$$\begin{pmatrix} T_{\text{gas}}^4 \\ T_{\text{sur}}^4 \end{pmatrix} = \frac{F_{\text{solar}}}{\sigma} \begin{pmatrix} 1 \\ 1 \cdot 1 - (-1) \cdot e^{-\tau} \end{pmatrix} \begin{pmatrix} 1 & -e^{-\tau} \\ 1 & 1 \end{pmatrix} \begin{pmatrix} 1 \\ 1 \end{pmatrix} ,$$

$$T_{\text{gas}} = \left( \frac{F_{\text{solar}}}{\sigma} \right)^{1/4} \left( \frac{1 - e^{-\tau}}{1 + e^{-\tau}} \right)^{1/4} , \quad (7.18)$$

$$T_{\text{sur}} = \left( \frac{F_{\text{solar}}}{\sigma} \right)^{1/4} \left( \frac{2}{1 + e^{-\tau}} \right)^{1/4} . \quad (7.19)$$

Thus, the greenhouse effect of a thin layer of gas raises the surface temperature by a factor  $[2/(1 + e^{-\tau})]^{1/4}$ , which has a maximum for  $\tau \rightarrow \infty$  of  $2^{1/4} \approx 1.19$ . It is a homework problem to compare this case to the case of two separate layers that are allowed to be at different temperatures, each with optical depth  $\tau/2$ . The combined effect of many infrared-absorbing layers can lead to dramatic increases in surface temperature, as in the case of Venus.

## 7.3 Vertical Structure

### 7.3.1 Adiabatic Lapse Rate

In a gravitationally-bound atmosphere density drops off rapidly with height, and a parcel of hot air that is displaced upwards quickly may actually find itself to be denser than its surroundings, even though it is hotter than its surroundings. The old adage “hot air rises” is only true if the density of the surrounding air falls off with height more slowly than does the density of an upwardly displaced parcel. A parcel will tend to conserve its heat as it moves, and will therefore adjust **adiabatically** to changes in atmospheric pressure. In order to determine whether an atmosphere is unstable to convection, we need to compare the drop off of the atmosphere’s temperature  $T$  with height  $z$ , called its **lapse rate**  $-dT/dz$ , to the **adiabatic lapse rate** that an ascending parcel will follow. If an atmosphere’s lapse rate is **superadiabatic**, that is, if its temperature falls off more rapidly

than for an ascending parcel, then the atmosphere is unstable to convection. On the other hand, if the atmosphere's lapse rate is **subadiabatic**, then it is stable and convection will not occur.

To derive an expression for the adiabatic lapse rate, we will assume that we are dealing with an ideal gas, such that:

$$p = \rho RT, \quad \text{or} \quad p v_s = RT, \quad (7.20)$$

where  $p$  is the pressure,  $\rho$  is the density,  $v_s \equiv \rho^{-1}$  is the specific volume,  $R$  is the gas constant, and  $T$  is the temperature. We know that an atmosphere in hydrostatic equilibrium has pressure decreasing with height, such that the gradient of the pressure divided by the density balances the force of gravity. Thus, a change in height is directly related to a change in pressure, and we need to know how a change in pressure is related to a change in density for our small parcel of fluid.

To find a relationship between changes in pressure and density we need to invoke the laws of thermodynamics. The first law of thermodynamics introduces the concept of **internal energy**  $E$ . If a small amount of energy is added slowly to a gas so that the pressure changes gradually, part of the energy will go into the work of expanding the gas, and the rest will go into the internal energy. The differential form describing the change in heat content is

$$dE + p dv_s. \quad (7.21)$$

If we first consider just the mathematics of the problem, then a theorem called **Pfaff's Theorem** tells us that for (7.21) there always exists an integrating factor and a perfect differential,  $dS$ , such that

$$dS = \frac{1}{T}(dE + p dv_s), \quad (7.22)$$

where  $1/T$  is the integrating factor. If the system is more complicated and involves more than two differentials, then without further information there is no mathematical certainty that an integrating factor and a perfect differential exist for the problem. However, it is observed experimentally that even in the case of three or more variables,  $1/T$  is still the integrating factor and  $dS$  is still the perfect differential. This means that the variable  $S$ , which is called the **specific entropy** ("specific" means "per unit mass"), is more than just a perfect differential. The term  $TdS$  describes the increase in heat content per unit mass, but when the concept of entropy was first introduced it was not known what physical quantity  $S$  measured. We now know that the entropy of a system is the logarithm of the number of quantum states accessible to the system, as discussed in Chapter 4.

The change of heat content  $TdS$  with respect to temperature is called the **specific heat**, and is denoted:

$$C_v \equiv T \left( \frac{\partial S}{\partial T} \right)_v = \left( \frac{\partial E}{\partial T} \right)_v, \quad (7.23)$$

when volume is held constant, and using (7.22) is denoted:

$$C_p \equiv T \left( \frac{\partial S}{\partial T} \right)_p = \left( \frac{\partial E}{\partial T} \right)_p + p \left( \frac{\partial v_s}{\partial T} \right)_p, \quad (7.24)$$

when pressure is held constant. For an ideal gas the internal energy is a function of  $T$  only, and for the case of constant  $C_v$ , (7.23) integrates to yield

$$E = C_v T. \quad (7.25)$$

With the equation of state (7.20), the second term on the right-hand side of (7.24) is simply the gas constant,  $R$ , and (7.24) reduces to

$$C_p = C_v + R. \quad (7.26)$$

With this (7.22) may be written

$$\begin{aligned} T dS &= C_v dT + p dv_s \\ &= C_v dT + p d \left( \frac{RT}{p} \right) \\ &= C_v dT + p \left( -\frac{RT}{p^2} dp + \frac{R}{p} dT \right) \\ &= C_p dT - \frac{RT}{p} dp. \end{aligned} \quad (7.27)$$

Adiabatic motion satisfies  $T dS = 0$  by definition. Such motion can also be called **isentropic motion** since it implies that entropy is conserved,  $dS = 0$ . Regardless of what we call it, for such motion (7.27) implies:

$$\frac{dT}{T} = \frac{R}{C_p} \frac{dp}{p}. \quad (7.28)$$

Integrating (7.28) (assuming constant  $R/C_p$ ) yields:

$$T = \theta \left( \frac{p}{p_0} \right)^{R/C_p},$$

or

$$\theta = T \left( \frac{p_0}{p} \right)^{R/C_p}, \quad (7.29)$$

where  $p_0$  is a reference pressure, and  $\theta$  is a reference temperature called the **potential temperature**. An atmosphere where potential temperature is constant with height has an adiabatic lapse rate. By (7.27) the relationship between entropy and potential temperature is:

$$dS = C_p d \log \theta. \quad (7.30)$$

Meteorologists tend to use potential temperature and astronomers tend to use entropy, but either is acceptable.

Notice that if we use the ideal gas law to eliminate  $T$  in (7.29), then for an adiabatic lapse rate we get a power-law relationship between pressure and density

$$\begin{aligned} \frac{p}{\rho R} &= \theta \left( \frac{p}{p_0} \right)^{R/C_p} \quad \Rightarrow \quad p^{1-R/C_p} \propto \rho, \\ \Rightarrow \quad p &= k \rho^{C_p/(C_p-R)} = k \rho^{(C_v+R)/C_v} = k \rho^{1+R/C_v}, \end{aligned} \quad (7.31)$$

where  $k$  is a constant of proportionality. A formula that connects pressure to density is called an **equation of state**. Interestingly, the equation of state that holds in Jupiter's interior is also a power law like (7.31), but of the form  $p = k\rho^2$ . Power-law equations of state are called **polytropes**.

To see how temperature drops off with height we now make the hydrostatic approximation

$$dp = -\rho g dz, \quad (7.32)$$

where  $z$  is the local vertical coordinate, and we assume for simplicity that the vertical range is small, such that  $g$  is approximately a constant. One should keep in mind that the problem can be easily worked out without this assumption and that for a “tall” atmosphere like Titan's it is not valid; we will return to the general case  $g = GM/r^2$  later in the chapter. Equation (7.28) yields a relationship between temperature and height:

$$dT = -\frac{g}{C_p} \frac{RT\rho}{p} dz = -\frac{g}{C_p} dz. \quad (7.33)$$

Therefore, the **dry adiabatic** temperature profile is  $g/C_p$ . For Earth this corresponds to about  $10 \text{ K km}^{-1}$ . However, this adiabatic profile does not exactly match the temperature gradient in Earth's lower atmosphere because of the presence of water vapor in the air. As a parcel of air rises it cools. Water vapor condenses and releases latent heat that keeps the atmosphere from achieving the dry adiabatic lapse rate. The actual lapse rate is about  $6 \text{ K km}^{-1}$  up to an altitude of about 15 km. This represents a **wet adiabatic** temperature profile.

We are now in a position to determine whether an atmosphere is stable or unstable to small vertical fluctuations. The vertical acceleration of our fluid volume satisfies the equation of motion:

$$\frac{d^2}{dt^2}(\delta z) = \frac{dw}{dt} = -g - \frac{1}{\rho} \frac{\partial p}{\partial z}, \quad (7.34)$$

where  $w$  is the vertical wind speed. We will apply the “parcel approximation” and assume that: i) the density of our fluid volume (parcel) may be different than its surroundings, but that ii) the pressure will always stay close to the environmental pressure, and that iii) there will be negligible exchange of heat between the fluid volume and the environment. Consider the case of a hot-air balloon. Pressure is just about continuous across the non-rigid walls of the balloon. Therefore, for the term  $\partial p/\partial z$  we can approximate with  $\partial \bar{p}/\partial z = -\bar{\rho}g$ , where  $\bar{\rho}$  is the background density. This yields

$$\frac{d^2}{dt^2}(\delta z) = -g \left( 1 - \frac{\bar{\rho}}{\rho} \right). \quad (7.35)$$

By further combining the parcel approximation,  $p = \bar{p}$ , with the ideal-gas law (7.20) and the definition of potential temperature (7.29), the ratio  $\bar{\rho}/\rho$  in (7.35) may be written  $\theta/\bar{\theta}$ , such that:

$$\frac{d^2}{dt^2}(\delta z) = -g \left( 1 - \frac{\theta}{\bar{\theta}} \right) = -g \left( \frac{\bar{\theta} - \theta}{\bar{\theta}} \right). \quad (7.36)$$

Next, we express the background potential temperature for a small vertical displacement  $\delta z$  as a Taylor series:

$$\bar{\theta}(\delta z) = \theta_0 + \frac{d\bar{\theta}}{dz} \delta z + \dots \quad (7.37)$$

We need one more detail from our balloon analogy. It is true that a balloonist needs to add heat to stay aloft only infrequently. A simple and fairly accurate assumption is thus to consider the case of no heat exchange, or adiabatic motion. In this case,  $\theta = \theta_0$ , and the equation of motion for the parcel becomes that of a simple harmonic oscillator:

$$\frac{d^2}{dt^2} \delta z = -\frac{g}{\bar{\theta}} \frac{d\bar{\theta}}{dz} \delta z \equiv -N^2 \delta z, \quad (7.38)$$

where  $N$  is called the **Brunt-Väisällä frequency**, or the **buoyancy frequency**, and is a measure of the stability of the atmosphere.

If  $N^2 > 0$  the fluid volume will oscillate about its initial level at the buoyancy frequency. Such waves are called gravity waves by meteorologists and g-mode waves by astronomers. If  $N^2 = 0$ , then the potential temperature is constant with height and the atmosphere is said to be neutrally stable. If  $N^2 < 0$ , then our calculation implies that the fluid volume will not be stable to small vertical displacements but will undergo unstable, convective motion. Since the case  $N^2 < 0$  implies that the background potential temperature is decreasing with height, the old adage “hot air rises” is still true if by “hot air” we mean “high potential temperature air.” An atmosphere whose lapse rate is larger than adiabatic, and hence unstable to convection, is said to have a **superadiabatic** lapse rate, and conversely, a stable atmosphere is said to have a **subadiabatic lapse rate**.

The bottom line is that hot *potential* air rises, cold *potential* air sinks. If temperature decreases with height faster than adiabatic lapse rate, convection will occur.

### 7.3.2 Lower Atmosphere

In the first 0.1 km of a terrestrial atmosphere the effects of daily surface heating and cooling, surface friction, and topography produce a turbulent region called the **planetary boundary layer**. Right at the surface, molecular viscosity forces the “no slip” boundary condition and the wind reduces to zero, such that even a weak breeze results in a strong vertical wind shear that can become turbulent near the surface. However, only a few millimeters above the surface molecular viscosity ceases to play a direct role in the dynamics except as a sink for the smallest eddies. The mixing caused by turbulent eddies is often parameterized as a diffusive process with an **eddy viscosity** that can be as much as a million or a billion times greater than the molecular viscosity. Much has been written about the pros and cons of approximating turbulence as a diffusive process. Although it is mathematically convenient to do so, turbulent mixing is a process that works first to

remove large-scale features and then proceeds slowly to remove small-scale features (this describes three-dimensional turbulence, like the breakup of a smoke ring, but not two-dimensional turbulence, for which mergers of small-scale features into large-scale features is the rule), whereas diffusion is a process that works first to remove small-scale features and then proceeds slowly to remove large-scale features. Nevertheless, the concept of eddy viscosity has allowed important progress to be made in problems where the energy spectrum of the turbulence is less important than the effects of overall mixing.

The temperature profile of an atmosphere in radiative equilibrium tends towards a superadiabatic (unstable) lapse rate, because the air near the ground gets warm and buoyant while the air overhead cools to space and gets heavy. The ensuing convection tends to relax the atmosphere back to the adiabatic (neutrally stable) lapse rate. Such is the case for the terrestrial atmospheres from their surfaces up to a point called the **tropopause** (“tropo” means “turning”). This layer of the atmosphere is called the **troposphere**, and contains most of the mass and most of the time-variable phenomena generally associated with the weather. On Earth the tropopause occurs in the altitude range 8-18 km; it is 10 km higher at the equator than at the poles. Anyone who has flown in a jet airplane knows roughly the height of the tropopause, because pilots announce it over the intercom: “Ladies and Gentlemen, we have reached our cruising altitude of 33,000 feet (10 km) and I’m turning off the seat belt sign, but...” Because of the exponential fall off of density with height, Earth’s troposphere contains 80% of the total atmospheric mass. It also contains most of the water vapor and consequently most of the clouds and stormy weather.

The hot surface of Venus prevents sulfur from being removed from the atmosphere and incorporated into the surface rocks. Sulfur dioxide ( $SO_2$ ) is abundant in Venus’s lower atmosphere. This provides a source of sulfur for the dense layer of sulfuric-acid clouds that exist between 50 and 80 km. Trace amounts of sulfur-bearing species can be detected in Earth’s atmosphere, especially following a major volcanic eruption. Although Mars has ample evidence for past volcanic activity, there has not been a detection of sulfur in its atmosphere.

On Venus, carbon dioxide and water vapor, along with sulfuric acid and sulfur dioxide, act to absorb essentially all of the infrared radiation emitted by the surface, causing an enormous 500 K increase in surface temperature above the planet’s effective temperature. The important greenhouse gases on Earth are water vapor and carbon dioxide. On Mars, carbon dioxide and atmospheric dust cause a greenhouse effect.

### 7.3.3 Middle Atmosphere

On Earth above the tropopause, the nearly adiabatic fall-off of temperature with height in the troposphere gives way to an *increase* of temperature with height. As we have already seen, this results in an extremely stable layer, called the **stratosphere** (“strato” means “layered”). Observations of persistent, thin layers of aerosol, and of long residence times for radioactive trace elements from nuclear explosions, are direct evidence of lack of mixing in the stratosphere.

The temperature continues to rise with altitude in Earth’s stratosphere until one reaches the **stratopause** at about 50 km. The source of heating in the stratosphere is the photochemistry of ozone ( $O_3$ ). Ozone concentrations peak at about 25 km. Ozone absorbs

ultraviolet light, and below about 75 km nearly all this radiative influx gets converted into thermal energy.

The chemistry of the stratosphere is complicated. Ozone is produced mostly over the equator but its largest concentrations are found over the poles, which implies that both dynamics and chemistry are important to the ozone budget. Mars also tends to have ozone concentrated over its poles, particularly over the winter pole. The dry Martian atmosphere has relatively few hydroxyl radicals to destroy the ozone.

Some of the most important chemical reactions in Earth's stratosphere are those that involve only oxygen. Photodissociation by solar ultraviolet radiation involves the reactions:



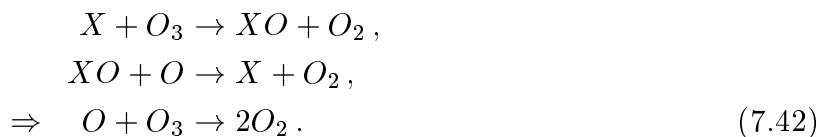
Three body collisions, where a third body  $M$  is required to satisfy conservation of momentum and energy, are described by



The reaction (7.40a) proceeds slowly and may be neglected for the stratosphere. The direct reaction



and the reaction (7.39a) either destroy or create “odd” oxygen ( $O$  or  $O_3$ ), and proceed at much slower rates than the reactions (7.39b) and (7.40b), which convert odd oxygen particles into each other. The equilibrium between  $O$  and  $O_3$  is controlled by the fast reactions, whose reaction rates and concentrations are altitude dependent. Other reactions that are important to the creation and destruction of ozone involve the minor constituents  $NO$ ,  $NO_2$ ,  $H$ ,  $OH$ ,  $HO_2$ , and  $Cl$ . An important destruction mechanism is the catalytic cycle:



On Earth, human activity has led to sharp increases in  $X = \{Cl, NO\}$  and subsequent sharp decreases in stratospheric ozone, most notably in the polar regions.

Above the stratopause, temperature again falls off with height, although at a slower rate than in the troposphere. This region is called the **mesosphere** (“meso” means “middle”). Temperatures fall off because there is less heating by ozone, and emission to space by carbon dioxide in the upper stratosphere and lower mesosphere provides an efficient cooling mechanism. The **mesopause** occurs at an altitude of about 80 km, marking the location of a temperature minimum of about 130 K. For many purposes, the stratosphere and mesosphere are taken together and referred to as simply the **middle atmosphere**.

The temperature profiles for the four giant planets have been determined by Voyager Spacecraft data, and Earth-based stellar occultation data. The Voyager data include occultations of the spacecraft's radio signal, and thermal data from the infrared interferometer spectrometer (IRIS). Each planet shows a tropopause and a stratosphere. Absorption of solar radiation by atmospheric gases probably does not account for all of the stratospheric heating, but a photochemically produced haze layer can absorb sufficient quantities of solar radiation to explain the temperature increase with height.

#### 7.3.4 Upper Atmosphere

As is the case for ozone in the stratosphere, above the mesopause, atomic and molecular oxygen strongly absorbs solar ultraviolet radiation and heats the atmosphere. This region is called the **thermosphere**, and temperatures rise with altitude to a peak that varies between about 500 and 2000 K, depending on solar activity. Just like the stratosphere, the thermosphere is stable to vertical mixing. At about 120 km, molecular diffusion becomes more important than turbulent mixing, and this altitude is called the **homopause** (or **turbopause**). Rocket trails clearly mark the homopause — they are rapidly mixed below it but linger relatively undisturbed above it. Molecular diffusion is mass dependent, and each species tends to fall off exponentially with its own scale height, leading to elemental fractionation that enriches the abundance of the lighter species at the top of the atmosphere.

At about 500 km, the mean free path grows to be comparable to the density scale height, marking the **exobase** and the start of the **exosphere**. At these high altitudes, sunlight can remove electrons from atmospheric constituents and form a supply of ions. These ions interact with a planet's magnetic field and with the solar wind to form a planet's **ionosphere**. On Earth, most of the ions come from molecular oxygen and nitrogen, while on Mars and Venus most of the ions come from carbon dioxide. Because of the chemistry, however, ionized oxygen atoms and molecules are the most abundant ion for all three atmospheres.

The structure of the thermospheres, exospheres, and ionospheres of the giant planets have been determined from optical and radio wavelength Voyager observations. The principal absorbers of ultraviolet light are  $H_2$ ,  $CH_4$ ,  $C_2H_2$ , and  $C_2H_6$ . The thermospheric temperatures of Jupiter, Saturn, and Uranus are about 1000, 420, and 800 K, respectively. The high temperature and low gravity on Uranus allows the atmosphere to extend out to the rings. This produces drag and shortens the lifetimes of dust particles. Since bands of dust were observed in the rings of Uranus, a source of dust must currently exist.

In general, the thermospheric energy budget is dependent on ionospheric processes. Even small energy inputs have a large effect on the structure. The auroral emissions discovered on Jupiter by Voyager were seen to be strong where the magnetic field lines from the orbit of Io intersect the atmosphere. The cascade of charged particles from Io can heat Jupiter's thermosphere to 1000 K. The energy sink for the thermosphere is conduction of heat *downwards* into the cooler layers below.

## 7.4 Escape Mechanisms

Mechanisms of volatile escape may be placed into two categories: thermal and non-thermal. Both processes provide the kinetic energy necessary for the volatile material to break free of the planet's gravity field and float away. Hydrogen is currently escaping from Earth and Venus primarily through the nonthermal mechanism of charge exchange between a hot proton and a thermal atom, where the resulting neutral hydrogen atom retains most of its kinetic energy and can easily escape. Both thermal and nonthermal escape rates are too small to have affected the composition of Earth's oceans.

A practical concept that we have already introduced is that of the exobase, which is defined to be the level in an atmosphere where the density scale height is equal to the horizontal mean free path. The exobase on Earth occurs at around 500 km. Above the exobase one enters the exosphere, where collisions are rare and molecules with velocities greater than the escape velocity tend to be lost to space. The nondimensional thermal-escape parameter  $\lambda$  is defined to be:

$$\begin{aligned}\lambda(r) &\equiv \frac{1}{k_B T} \frac{GMm}{r}, \\ &= \frac{r}{H} = \left(\frac{v_e}{U}\right)^2,\end{aligned}\tag{7.43}$$

where  $M$  and  $m$  are the mass of the planet and molecule, respectively ( $H$  is the vertical scale height,  $v_e$  is the escape velocity, and  $U$  is the thermal velocity, defined below). We denote the value of  $\lambda$  at the exobase as  $\lambda_{\text{ex}}$ . In general, a low value of  $\lambda_{\text{ex}}$  indicates a hot gas in a weak gravity field. It turns out that the extremely low value  $\lambda_{\text{ex}} = 2$  implies a supersonic flow. On the Sun this corresponds to the solar wind. The solar-wind mechanism may have occurred on the planets early in their history when they had hot enough atmospheres, in which case it is referred to as “blow off” or “hydrodynamic escape.” For this mechanism, the temperature and density profiles cannot be treated as given, but must be determined as part of the problem.

The value of  $\lambda_{\text{ex}}$  for hydrogen is sensitive to the variable exobase temperature, but is typically  $\lambda_{\text{ex}} \approx 8$  in Earth's atmosphere. However, Earth's exospheric structure is controlled by oxygen atoms, for which  $\lambda_{\text{ex}} \approx 16 \times 8 = 128$ .

### 7.3.1 Jean's Escape

For large values of  $\lambda_{\text{ex}}$ , a process known as **Jean's escape** becomes important. Consider an exosphere in hydrostatic balance, with particle number density  $n = \rho/m$ :

$$dp = -\rho g dr = -nm \frac{GM}{r^2} dr.\tag{7.44}$$

We assume an isothermal ( $dT/dr = 0$ ) exosphere and may write the ideal-gas law as

$$dp = k_B T dn.\tag{7.45}$$

Then we eliminate  $dp$  from (7.44) and (7.45) to get

$$\frac{dn}{n} = -\frac{GMm}{k_B T} \frac{dr}{r^2}. \quad (7.46)$$

Next, we integrate (7.46) to yield

$$\begin{aligned} \log(n/n_{\text{ex}}) &= \frac{GMm}{k_B T} \left( \frac{1}{r} - \frac{1}{r_{\text{ex}}} \right) = \lambda(r) - \lambda_{\text{ex}}, \\ \Rightarrow n(r) &= n_{\text{ex}} e^{\frac{GMm}{k_B T} \left( \frac{1}{r} - \frac{1}{r_{\text{ex}}} \right)} = n_{\text{ex}} e^{\lambda(r) - \lambda_{\text{ex}}}. \end{aligned} \quad (7.47)$$

For small ranges of vertical distance, it is customary to set  $r = r_{\text{ex}} + z$ , and expand the function  $1/r$  in the exponent of (7.47) as a Taylor series, to get the familiar form  $-z/H$ , where  $1/H = (GMm/r_{\text{ex}}^2)/k_B T$  is the inverse of the density scale height. In the exosphere, each gas of different mass obeys its own version of (7.47).

If  $\lambda_{\text{ex}}$  is not too small, the escape rate is not too large and the velocity distribution may be described using the same statistical Boltzmann factor that we used in the discussion of blackbody radiation. Here the appropriate energy is  $E = mv^2/2$ . We will estimate the total flux of molecules escaping by assuming that it is equal to the upward flux of molecules through the exobase that have velocities at or greater than the escape velocity,  $v_e$ . The number of molecules per unit volume,  $dn$ , that have three-dimensional velocities  $\mathbf{v}$  with magnitudes between  $v$  and  $v + dv$  is:

$$\begin{aligned} dn &= n_{\text{ex}} \frac{e^{-(mv^2/2k_B T)} v^2 dv}{\int_0^\infty e^{-(mv^2/2k_B T)} v^2 dv}, \\ &= n_{\text{ex}} \frac{4}{\sqrt{\pi}} U^{-3} e^{-(v/U)^2} v^2 dv, \end{aligned} \quad (7.48)$$

where  $U \equiv (2k_B T/m)^{1/2}$  is the thermal velocity, and we have used  $\int_0^\infty e^{-x^2} x^2 dx = \sqrt{\pi}/4$ . Analogous to the solid-angle considerations in our previous discussion on blackbody radiation, the flux  $\dot{N}$  (number per unit area per unit time) moving upward is obtained by multiplying  $dn$  by  $v/4$ . The total flux of escaping molecules is found by integrating from the escape velocity  $v = v_e = (2GM/r)^{1/2}$  to  $v = \infty$ :

$$\dot{N} = n_{\text{ex}} \frac{1}{\sqrt{\pi}} U^{-3} \int_{v_e}^\infty e^{-(v/U)^2} v^3 dv. \quad (7.49)$$

By setting  $y = (v/U)^2$  in (7.49), such that  $v^3 dv = (U^4/2) y dy$ , and integrating by parts, the escape flux is

$$\dot{N} = \frac{1}{2} n_{\text{ex}} \frac{U}{\sqrt{\pi}} \int_{\lambda_{\text{ex}}}^\infty e^{-y} y dy = B \frac{1}{2} n_{\text{ex}} \frac{U}{\sqrt{\pi}} (1 + \lambda_{\text{ex}}) e^{-\lambda_{\text{ex}}}. \quad (7.50)$$

We have used  $\lambda_{\text{ex}} = (v_e/U)^2$ , and have inserted a factor  $B \approx 0.75$  in the final answer to account for the fact that the high-velocity tail of the velocity distribution is depleted by the escape process.

Equation (7.50) is known as **Jean’s equation**. The presence of the factor  $B$  reminds us that the derivation of (7.50) is approximate. A typical calculation of the escape flux at Earth’s exobase, for atomic hydrogen  $H$  and low solar activity, is

$$T \approx 900 \text{ K}, \quad \lambda_{\text{ex}} \approx 8, \quad n_{\text{ex}} \approx 10^5 \text{ cm}^{-3}, \quad B \approx 0.75,$$

yielding

$$\dot{N} \approx 6 \times 10^7 \text{ cm}^{-2} \text{ s}^{-1}.$$

The escape flux from nonthermal processes is larger than this value for the present-day Earth. If the current total escape flux from thermal and nonthermal processes is applied over the age of the solar system, the loss of hydrogen from Earth is equivalent to only a few meters of liquid water. However, the flux could have been much higher in the past, because it is sensitive to the structure of the atmosphere. The negative exponential dependence of Jean’s escape on the molecular mass implies that heavier molecules escape at a much slower rate than lighter molecules, which leads to elemental fractionation in the upper atmosphere.

#### 7.4.2 Nonthermal Escape

Nonthermal escape processes account for most of the present escape flux for Earth, and the same is most likely true for Venus. They are also invoked as the explanation for the 75% enrichment of the  $^{15}\text{N}/^{14}\text{N}$  ratio in the Martian atmosphere. Except for photodissociation, all the important nonthermal escape mechanisms involve charged particles. Charged particles get trapped by magnetic fields and therefore do not readily escape. However, a fast proton can collide with a slow hydrogen atom and take the electron from the hydrogen atom. This charge-exchange process changes the fast proton into an electrically neutral hydrogen atom, but does not significantly diminish its kinetic energy. If after such a collision the fast, neutrally charged hydrogen atom is moving upwards, it is likely to escape.

Another important nonthermal escape process is chemical and photochemical dissociation. Either excess energy of reaction, or excess energy of the bombarding photon or electron, is converted into kinetic energy in the dissociated atoms. A common effect of electrical discharges of a kilovolt or more is “sputtering,” where several atoms can be ejected from the spark region at high velocities. If an ion is formed very high in the atmosphere, it can be swept out of a planet’s atmosphere by the solar wind. This is particularly important for Io, where ions are swept away by Jupiter’s magnetic field.

### 7.5 Volatile Inventories

The terrestrial planets Venus, Earth, and Mars have present-day atmospheres that are intriguingly different. The atmospheres of Venus and Mars are both primarily  $\text{CO}_2$ , but represent two extreme fates in atmospheric evolution: Venus has a dense and hot atmosphere, and Mars has a thin and cold atmosphere. One can wonder if Earth is ultimately headed towards one or the other of these fates. One can also wonder whether these three atmospheres have always been so different.

The history of volatiles on the terrestrial planets includes their origin, their interactions with refractory material, and their rates of escape into space. During the initial accretion and formation of the terrestrial planets, it is thought that most or all of the original water reacted strongly with the iron to form iron oxides and hydrogen gas, with the hydrogen gas subsequently escaping to space. Until the iron cores in the planets were completely formed and this mechanism was shut down, the outflow of hydrogen probably took much of the other solar-abundance volatile material with it. Thus, one likely possibility is that the present-day atmospheres of Venus, Earth, and Mars are not primordial, but have been formed by outgassing and by cometary impacts that have taken place since the end of core formation.

The initial inventory of water that each terrestrial planet had at its formation is a debated question. One school of thought is that Venus formed in an unusually dry state compared with Earth and Mars, another is that each terrestrial planet must have started out with about the same amount of water per unit mass. The argument for an initially dry Venus is that water-bearing minerals would not condense in the high-temperature regions of the protoplanetary nebula, inside of about 1 AU. Proponents of the opposite school of thought argue that gravitational scattering caused the terrestrial planets to form out of materials that originated over the whole range of terrestrial-planet orbits, and therefore that the original water inventories for Venus, Earth, and Mars should be similar.

An important observable that bears on the question of original water is the enrichment of deuterium relative to hydrogen. A measurement of the D/H ratio yields a constraint on the amount of hydrogen that has escaped from a planet. In order for the D/H ratio to be useful, one needs to estimate the relative importance of the different hydrogen escape mechanisms and the original D/H ratio for the planet. In addition, one needs an idea of the hydrogen sources available to a planet after its formation, like cometary impacts.

The initial value of D/H for a planet is not an easy quantity to determine. A value of  $0.2 \times 10^{-4}$  has been put forward for the protoplanetary nebula, which is within a factor of two or so for the present-day values of D/H inferred for Jupiter and Saturn. However, the D/H ratio in Standard Mean Ocean Water (SMOW) on Earth is  $1.6 \times 10^{-4}$ , which is also about the D/H ratio in hydrated minerals in meteorites, and is larger by a factor of eight over the previously mentioned value. At the extreme end, some organic molecules in carbonaceous chondrites have shown D/H ratios as high as  $20 \times 10^{-4}$ . The enrichment found in terrestrial planets and most meteorites over the protoplanetary nebula value could be the result of exotic high D/H material deposited on the terrestrial planets, or it could be the result of massive hydrogen escape from the planets early in their lifetimes through the hydrodynamic blow-off mechanism. In any event, we will assume that any enrichment mechanism acting on the initial planets and meteorite parent bodies affected each equally, and take the Earth ocean value of  $1.6 \times 10^{-4}$  as the initial D/H ratio.

### 7.5.1 Water on Venus

The amount of water in the atmosphere of Venus is currently about  $10^{-5}$  of that in Earth's oceans. The D/H ratio is an important diagnostic of the history of water on a planet. The Pioneer Venus mission provided two different observations of D/H for Venus. An ion with mass 2 was observed in some detail in the ionosphere, and it was argued on the

basis of its chemical behavior that this ion was  $D^+$ , rather than  $H_2^+$ . If the identification is correct, the observation implies  $D/H \approx 100 \times 10^{-4}$  in the bulk atmosphere. A second observation comes from examining water-related peaks observed by the Pioneer Venus Large Probe mass spectrometer. Accidentally, large drops of Venusian water found their way into the mass spectrometer as the Large Probe descended from 50 to 26 km altitude. Although this ruined part of the altitude profile, it did provide a direct measurement of the D/H ratio near the equator for Venus:  $D/H = 160 \pm 60 \times 10^{-4}$ . Thus, the D/H ratio on Venus is two orders of magnitude larger than on Earth.

If the water on Venus has not been replenished over its lifetime, and Earth and Venus started out with the same amount of water, then the 100-fold enhancement of D/H on Venus relative to Earth implies that Venus once had 100 times more water than it now has. The standard explanation for this is the so-called “run-away greenhouse” theory, which holds that Venus was never cool enough to condense liquid water on its surface. Instead, the water was held in the form of steam in the atmosphere, and the high-altitude steam was photodissociated into hydrogen, which then escaped.

The above scenario provides a self-consistent explanation for the high present-day D/H ratio and low water abundance on Venus. Recently, it has been suggested that water on Venus is in steady state, with outgassing and cometary impacts balancing loss of hydrogen to space. In fact, the high D/H ratio on Venus can be explained to within the measurement error by the slow, nonthermal hydrogen-escape mechanisms currently operating on Venus. This means that it is not necessarily true that the D/H ratio implies that Venus once had a factor of 100-times more water than it currently has. A completely satisfactory picture that explains all the observations for Venus has yet to emerge.

### 7.5.2 Water on Mars

The present-day Mars is a cold and dry desert planet. The global mean surface pressure is about 7 mbar. The thin atmosphere does not raise the surface temperature more than about 5K over the effective temperature of 212K. During the warmest part of the day, temperatures may slightly exceed the freezing point of water, but the low pressures cause water vapor to evaporate quickly, and water in the liquid phase on the surface of Mars is not stable.

Nevertheless, Mariner 9 discovered channels that resemble dried river channels on Earth, and were most likely carved by running water. Some of these **fluvial** channels appear to be the result of brief but catastrophic outflows of liquid water, whereas others show gullies and valley networks that indicate that liquid water probably existed for an extended period of time at some point early in Mars’ history.

There is also geomorphological evidence that the older craters on Mars are much more eroded than the younger craters, suggesting that the atmosphere was once much thicker than it is at present. Models of a thick  $CO_2$  atmosphere on Mars show that the resulting greenhouse effect could have kept the surface temperature above the freezing point of water for as long as  $10^9$  years.<sup>2</sup> One future test of the warm-climate hypothesis will be the

---

<sup>2</sup> For details on such models, see the paper “The Case for a Wet, Warm Climate on Early Mars,” by Pollack, Kasting, Richardson, and Poliakoff, *Icarus* **71**, 203–224, 1987.

search for minerals on the surface of Mars that would have been produced by wet chemical weathering, such as clays and carbonates.

### 7.5.3 CO<sub>2</sub> on Mars

One of the classical papers in planetary science that has stood the test of time is “Behavior of Carbon Dioxide and Other Volatiles on Mars,” by Leighton and Murray (1966). At the time that this paper appeared, the common wisdom was that the Martian polar caps were made of water ice. However, Leighton and Murray considered the heat balance of the planet with a model for the diurnal (daily) and annual variations of the surface and soil temperatures as a function of latitude, together with evidence that the surface pressure was in the millibar range, and that water vapor was a minor constituent relative to CO<sub>2</sub>. They found evidence that CO<sub>2</sub> should condense in large quantities at the poles, and that the poles and atmosphere should be in solid-vapor equilibrium with CO<sub>2</sub> as the only active phase.

The detailed calculations showed that this model could explain the seasonal appearance and disappearance of the polar caps. In fact, the surface pressure changes by 20% from season to season as the polar ice grows and recedes, resulting in a poleward wind (the pressure drop experienced while flying in the pressurized cabin of a jet airplane is also about 20%). High-resolution images of the Martian polar caps reveal intriguing spiral patterns and layered terrain. Although Mars currently has an obliquity of 24°, very similar to Earth’s, it is known that both the Martian obliquity and eccentricity have large, long-term chaotic variations that may have a dramatic effect on the planet’s climate, and may help to explain the layering in the polar caps.

It is not known definitively why the atmosphere of Mars underwent a dramatic decrease in pressure, from perhaps a few bars in its first 10<sup>9</sup> years, to about 7 mbar at present. One idea is that weathering of surface rocks removed CO<sub>2</sub> from the atmosphere, locking the carbon into carbonate rocks, as has occurred on Earth. This process can eliminate a several-bar CO<sub>2</sub> atmosphere on Mars in only about  $5 \times 10^7$  years for a surface temperature of 273 K, indicating that it would be difficult to maintain a wet, warm climate on Mars over the age of the solar system. A similar process also affects the carbon budget of Earth. About 60 bar of carbon is presently tied up in carbonate rocks on Earth. It is likely that Earth’s atmosphere once contained significantly more CO<sub>2</sub> than it does at present, and that atmospheric temperatures were once higher. A major difference between Earth and Mars is that plate tectonics on Earth continuously recycles carbon, whereas carbon is locked into the rocks and polar caps on Mars.

## 7.6 VENUS

Venus is a slowly rotating planet ( $\tau = 243$  days), and so is Titan ( $\tau = 16$  days rotation period). Both have atmospheres that are denser than Earth’s, and both display a curious superrotation in their atmospheres that has yet to be explained. Venus has been extensively observed by the Pioneer and Venera spacecraft and by ground-based observations. In contrast, Titan has been closely scrutinized only once, by the Voyager 1 spacecraft on November 12, 1980.

To examine the surface of Venus in detail one must first see past the hottest and densest terrestrial atmosphere in the solar system. At the 1991 DPS conference (“DPS” stands for Division for Planetary Sciences of the American Astronomical Society), it was announced that the atmosphere of Venus is partially transparent at a wavelength of 1  $\mu\text{m}$ . This discovery of a “window” in the Venusian atmosphere is significant because for the most part the atmosphere is opaque to short-wave radiation. Ground-based and spacecraft observers have had to struggle to determine the 243 days rotation period and  $< 3^\circ$  inclination of Venus. The key has been radar, which has a long enough wavelength to penetrate the Venusian atmosphere. The Magellan radar mapper was designed to exploit this transparency to long-wave radiation and successfully mapped the entire surface at high resolution.

Atmospheric scientists studying Venus have not been frustrated by a lack of data like their geological colleagues; on the contrary, there is a wealth of atmospheric data from decades of ground-based and spacecraft observations. Some of the atmospheric topics of particular interest are the bulk composition, the sulfuric acid clouds, the ultraviolet (UV) markings, the “4-day” wind, the meridional wind, the polar vortex, the convective and stable layers, the differences between the night side and day side, and the occurrence of lightning.

### 7.6.1 Bulk Composition

We have both spectroscopic and *in situ* observations that tell us about the chemical makeup of the Venusian atmosphere. Early spectroscopic observations were incorrectly interpreted as evidence for water vapor on Venus; it was later shown that the water vapor in Earth’s atmosphere accounted for the signal. In 1932, Adams and Dunham used the Mount Wilson 100-inch reflector to detect several bands in the near infrared that they correctly attributed to  $\text{CO}_2$  gas in the atmosphere of Venus. In fact,  $\text{CO}_2$  (96.5%) and a small amount of  $\text{N}_2$  (3.5%) account for 99.9% of the atmosphere of Venus below 80 km. In addition, there are positive identifications of  $\text{CO}$ ,  $\text{O}_2$ , and  $\text{O}$  — the expected products of chemical reactions involving  $\text{CO}_2$ . Earth-based spectroscopy has also established that the bright clouds on Venus are composed of concentrated sulfuric acid ( $\text{H}_2\text{SO}_4$ ).

Earth-based observations gave way to *in situ* measurements in December, 1978, when the spacecraft Venera 11, 12, and Pioneer Venus each dropped probes into the atmosphere. These probes contained mass spectrometers, gas chromatographs, optical spectrometers, ion spectrometers, and additional instruments designed to measure ion densities and cloud properties. The role of  $\text{N}_2$  as the second major atmospheric constituent was established, and the trace abundances of the noble gases Ne, Ar, and Kr were determined. The major sulfur-bearing gas was determined to be  $\text{SO}_2$ , rather than COS.

### 7.6.2 Sulfuric Acid Clouds

Apart from the dark shadow on the night side of Venus that causes phases as seen from Earth, Venus is featureless in visible wavelengths. It was clear early on that Venus was completely covered by a highly reflective layer of clouds. The polarization of light from Venus was observed to be different than one would expect from simple Rayleigh scattering, implying that the cloud particles have a strong effect on the optical properties

of the atmosphere. In fact, it was realized that the polarization data implied that the clouds are composed of spherical particles, which have a distinctive variation of polarization with observing angle, as described by **Mie theory**. Numerical calculations of multiply scattering spheres indicated that the cloud particles on Venus have an average radius of about  $1\ \mu\text{m}$ , and an index of refraction of about 1.45. Together with this geometrical and optical information, spectroscopic observations made in the late 1960's and early 1970's revealed broad absorption features at  $\approx 0.3$ , 3, and  $11.2\ \mu\text{m}$ . Given the above constraints, Sill (1972) and Young and Young (1973) independently identified the cloud particles as uniform droplets of concentrated sulfuric acid, with a concentration of 75% by weight. The sulfuric acid clouds extend from about 47.5 to 70 km in altitude.

### 7.6.3 Ultraviolet Markings

Although bland at visible wavelengths, Venus does show variable cloud features in the ultraviolet (UV), as first reported in the late 1920's. A dark "horizontal Y" pattern is seen to appear and disappear with about a 4-day period. Sometimes one pole or the other will brighten and stay bright for months. Spacecraft images reveal that, along with these planetary-scale features, there are also small but discernible km-sized features in the clouds.

It is not known whether the smaller features are caused by the same mechanism as the planetary-scale features, or even what the UV absorber is. In 1979, sulfur dioxide ( $\text{SO}_2$ ) was discovered on Venus by Earth-based observations, by Pioneer Venus ultraviolet observations and *in situ* probe measurements, and by the International Ultraviolet Explorer (IUE) satellite. Sulfur dioxide can account for the contrast of the dark features and the mean reflectance of the atmosphere, but only for wavelengths shorter than  $3200\ \text{\AA}$  ( $0.32\ \mu\text{m}$ ). A second absorber, possibly amorphous sulfur, is required to explain the patterns seen at longer wavelengths. Both chemical and dynamical mechanisms have been proposed to explain the patterns themselves, but there is not yet a clear consensus on what causes them.

### 7.6.4 The 4-day Wind

While it was known since the late 1920's that Venus showed cloud features in the UV, and in the 1960's that these features exhibited a 4-day periodicity, the Earth-based observations did not have the resolution necessary to determine whether the features were evidence of planetary-scale waves or a bulk rotation of the atmosphere.

Planetary spacecraft from Mariner 10 to Galileo have sent back UV images of Venus with excellent spatial and temporal resolution. By tracking small cloud features in these images, the distinction between waves and winds can be made. The 4-day periodicity of the large-scale features is seen to also be present in the small-scale features, implying a cloud-top wind speed at the equator of about  $100\ \text{ms}^{-1}$ . This "4-day wind" moves in the **retrograde** direction, which is the same direction as the solid planet rotates, but over sixty times faster (recall that the planet rotates once in 243 days).

Finding an explanation for the superrotation of the atmosphere of Venus is one of the key unsolved problems in atmospheric dynamics. One proposed mechanism involves

pumping up the winds with the energy from solar tides. Another invokes vertically propagating gravity waves. As gravity waves travel upwards, they tend to increase in amplitude as the density decreases, until finally they “break,” in much the same way as ocean waves break on a beach. The momentum carried upwards by the waves gets deposited at the level where they break, thereby pumping up the zonal wind.

The zonal-wind profile  $\bar{u}(y)$  during the nominal Pioneer Venus mission showed a  $\cos(y)$  dependence characteristic of solid-body (constant angular velocity) rotation. However, during the Mariner 10 encounter, midlatitude winds were significantly stronger than for the case of solid-body rotation. Such a time-variable midlatitude jet is not unexpected on a terrestrial planet, given our experience with the variability of Earth’s atmosphere, but it stands in contrast to the long-term stability of the zonal-wind profiles seen on the giant planets.

The large-scale patterns tend to remain coherent even though the winds determined from small-scale features are often variable and asymmetric about the equator. This implies that the horizontal-Y pattern is controlled by planetary-scale waves. It happens that the phase speeds of these waves are slow compared to the wind speed, so that they are both circling the planet with about a 4-day period.

Below the clouds, Doppler tracking of entry probes has revealed that the zonal-wind speed decays from about  $100\text{ms}^{-1}$  in the cloud region to zero at the surface, in a fairly monotonic manner. Above the clouds it is difficult to accurately determine wind speeds. One method is to observe the Doppler shifts in weak spectral lines. The zonal wind apparently also dies off with altitude above the cloud tops, transitioning into a simpler subsolar-to-antisolar flow at about 100 km altitude.

### 7.6.5 The Meridional Wind

Terrestrial planets tend to receive more sunlight at their equators than at their poles. In response to this differential heating, a so-called Hadley cell circulation develops whereby air rises at the warm equator and moves poleward, and when it reaches the pole it descends and returns along the ground towards the equator. As we will see in the next chapter, the Coriolis force on rapidly rotating planets like Earth and Mars acts to deflect the Hadley cell’s purely meridional flow into a more zonal flow. In contrast, Venus is a slowly rotating planet, and one might expect the atmospheric motion to be dominated by a simple Hadley cell. Venus does indeed exhibit some of the largest persistent meridional (north-south) winds of any planet. A poleward flow of about  $10\text{ms}^{-1}$  exists in each hemisphere at the cloud level. However, the Hadley circulation does not dominate the atmospheric motion, but instead the 4-day zonal wind combines with the meridional wind to produce an intriguing spiral pattern around each pole on Venus.

### 7.6.6 Lightning

In the late 1950’s Venus was shown to emit bursts of radio signals, and one theory held that these were evidence for lightning in the atmosphere of Venus. Other explanations besides lightning were equally plausible, however, including the high frequency radio emissions that a hot planetary surface and lower atmosphere can emit.

The Venera 11 and 12 probes each had an experiment called “Groza,” the Russian word for thunderstorm, specifically designed to detect evidence for lightning. Also, the Pioneer Venus plasma wave instrument had a limited capability to detect whistler-mode radio signals. In December, 1978 the Groza instruments on the two Venera probes detected a large number of magnetic pulses of the type usually associated with distant lightning on Earth, and shortly afterwards the plasma wave detector orbiting overhead on Pioneer Venus detected similar electrical pulses. It is almost certain that these electromagnetic pulses were the result of lightning flashes on Venus, although there are no photographs of the lightning flashes themselves. The signal characteristics suggest that the lightning flashes occurred about 1200 to 1500 km from the probes, and had a horizontal extent of about 120 to 150 km. These dimensions are similar to large thunderstorm fronts on Earth. The Venera 11 probe followed the Venera 12 probe by four days into the same equatorial region of the planet. The lightning activity detected by Venera 11 was significantly greater than that detected by Venera 12, implying that lightning on Venus is sporadic, just like it is on Earth. The apparent whistler-mode sources were clustered near Phoebe, Beta, and Atla Regios, suggesting a possible link with volcanic activity.

## 7.7 TITAN

Saturn’s satellite Titan has the densest atmosphere of any terrestrial planet save Venus, and it is the only satellite with a thick atmosphere. With a radius of  $2575 \pm 0.5$  km, Titan is second only to Ganymede in size among the satellites, and both are bigger than the planet Mercury. Titan’s atmospheric surface pressure is  $1.496 \pm .02$  bar, or 50% greater than the surface pressure on Earth. The radius and surface pressure are known accurately from the Voyager 1 radio occultation experiment. Like Earth, Titan’s atmosphere is composed primarily of  $N_2$ . In contrast, both Venus and Mars have atmospheres that are composed primarily of  $CO_2$ .

### 7.7.1 Sacrifice Fly

Much of what we know about Titan comes from the Voyager 1 encounter with the satellite on November 12, 1980. To encounter Titan, the Voyager 1 spacecraft had to be diverted from the path that would have taken it on to Uranus and Neptune. An encounter with Titan was considered so important by the Voyager mission planners that, if the Voyager 1 encounter had failed, the Voyager 2 spacecraft was also slated to be sent to Titan instead of on to Uranus and Neptune. Because everything worked well, the two Voyager spacecraft were able to take different paths and give us both a Titan encounter and a “Grand Tour” of all four gas giants.

### 7.7.2 Aerosol Haze

Titan is covered with a brown, smoggy haze layer that is so thick that Voyager 1 was unable to image the satellite’s surface, or even see cloud features. In 1944, Kuiper discovered  $CH_4$  on Titan from Earth-based spectroscopy. Voyager 1 discovered at least nine organic molecules heavier than methane in Titan’s atmosphere, including ethane ( $C_2H_6$ ), propane ( $C_3H_8$ ), acetylene ( $C_2H_2$ ), ethylene ( $C_2H_4$ ), hydrogen cyanide (HCN),

and molecular hydrogen ( $\text{H}_2$ ). The aerosols that make up the haze are thought to be the end products of methane photochemistry. The optical properties of Titan's haze suggests that these aerosol particles are not spherical, but are oblong in shape. The solar heating of the aerosols produces a stable layer that aids in the formation of complicated organic molecules in a self-sustaining manner.

### 7.7.3 Atmospheric Composition

Titan's outer atmosphere is well studied because of the information provided by the Voyager 1 ultraviolet spectrometer (UVS). The UVS instrument observed the Sun through Titan's atmosphere, and the resulting spectrum provided a direct indication that Titan's atmosphere is primarily composed of  $\text{N}_2$ . The Voyager radio occultation experiment yielded a profile of the ratio of temperature to mean molecular weight, which when combined with the Voyager infrared (IRIS) temperature results yielded a mean molecular weight of just over 28. This further supports the idea that the atmosphere is dominated by  $\text{N}_2$ . The large amount of nitrogen in Titan's atmosphere probably comes from photochemical decomposition of  $\text{NH}_3$  in a hot primordial atmosphere. An important source for the upper-atmosphere haze particles besides  $\text{CH}_4$  photochemistry which provides a continual source of  $\text{H}_2$  that replenishes that lost from the atmosphere. The molecular hydrogen abundance represents a balance between production and escape. Another contributor to atmospheric haze may be HCN molecules formed by  $\text{N}_2$  photochemistry.

### 7.7.4 Vertical Structure

Assuming a pure nitrogen atmosphere, the Voyager radio occultation experiment indicates that the surface temperature of Titan is  $94.0 \pm 0.7$  K. The surface pressure is about 1.5 bar. Temperature decreases with altitude with a lapse rate of  $1.38 \pm 0.10$  K  $\text{km}^{-1}$ , which is quite close to the adiabatic lapse rate expected for an  $\text{N}_2$  atmosphere. At 42 km altitude the temperature reaches a minimum of 71 K. This level is the tropopause, and acts like a cold trap for the organic material in the atmosphere. The temperature above the tropopause rises fairly quickly to 160 – 175 K at 200 km altitude, about 80K higher than at the surface. The temperature then stays constant with height all the way out to the exosphere at about 1600 km. The rapid heating of the stratosphere of Titan is due to ultraviolet solar radiation incident in the upper atmosphere. The absorption of UV radiation contributes to the photochemical processes discussed above.

Titan has a “tall atmosphere” in the sense that the gravitational acceleration drops by more than a factor of two between the surface and the exosphere. The high temperatures and weak gravity in the upper atmosphere combine to make hydrogen escape very efficient. An extensive atomic hydrogen torus circling Saturn in the same orbit as Titan was detected in Lyman  $\alpha$  by the Voyager UVS instrument.

The haze encountered by Voyager 1 obscured any observations of underlying clouds. Nitrogen clouds are not thought to be likely, because the temperature only approaches the condensation temperature of nitrogen at around 30 km altitude, and there it is about 5K too high for nitrogen to condense. Methane clouds are a possibility, however. The radio occultation signal showed unusually strong scintillations (fluctuations) in the pressure range between 0.2 and 0.8 bar. One possibility is that the scintillations are caused by

layered clouds in Titan's atmosphere, but other explanations have been put forward, like vertically propagating gravity waves.

#### 7.7.5 Ethane Lakes

One of the most interesting predictions for Titan is that its surface may be covered with lakes of liquid ethane. An early prediction of an entire ocean of ethane has been ruled unlikely as the result of Earth-based radar studies. Ethane is the most abundant product from the methane photochemistry occurring in the stratosphere. The fate of most of the aerosol particles in Titan's haze layer is to fall out as black, tar-like rain, and to collect as a layer of organic tar on the surface. But ethane should be liquid on Titan's surface, and calculations of the amount of ethane produced by photochemistry over the age of the solar system suggest that lakes of ethane are a distinct possibility. Radar signals are quite sensitive to the difference between solid and liquid surfaces. Attempts have been made to bounce radar signals off of Titan from Earth, but so far the results have been inconclusive. The planned radar mapping of Titan's surface by the Cassini orbiter should indicate whether or not ethane lakes actually exist on its surface.

#### 7.7.7 The Cassini Mission

The upcoming Cassini mission to the Saturnian system has been described humorously as “a mission to Titan and its planet Saturn.” The Cassini mission is a joint project between NASA and the European Space Agency (ESA). ESA is in charge of an atmospheric probe that will descend into the atmosphere of Titan and make the first *in situ* measurements. NASA is in charge of the Cassini Saturn orbiter, which will map the surface of Titan using a radar technique similar to that employed by the Magellan spacecraft at Venus, as well as carry out many other observations of Titan, Saturn, and Saturn's rings with its high-precision ultraviolet, visible, infrared, and radio-frequency detectors.

### 7.8 Mars

### 7.9 Io

### 7.10 Triton and Pluto/Charon

Triton's surface is covered by a mixture of solid nitrogen and trace amounts of methane and carbon monoxide. These constituents also compose the atmosphere. Triton showed evidence for active plumes during the Voyager 2 flyby. Pluto's surface has a similar composition as Triton but it has less nitrogen and about twice as much methane.

### 7.11 Earth

### 7.12 Jupiter and Saturn

We expect the interiors of Jupiter, Saturn and Neptune to be vigorously convecting in order to transport internal heat to their surfaces, where it is eventually radiated to space.

Since only a small superadiabaticity is required for effective convection, an unstable atmosphere tends to develop a lapse rate that is only marginally larger than the adiabatic lapse rate. The vertical temperature profiles of the giant planets are observed to be adiabatic at depth, to within measurement error.

In an adiabatic planet, small temperature fluctuations are efficiently removed by self-regulating convection. This is taken as the explanation for the remarkable lack of temperature variation seen on the surfaces of the giant planets. Even though the solar insolation varies by a sizeable factor from equator to pole, the observed equator-to-pole temperature differences are only a few degrees, in sharp contrast to the many tens of degrees seen on Earth. Apparently, the adiabatic interiors of the giant planets act as a short circuit by arranging for more internal heat to come out at the poles than at the equator, in just the right proportion to balance the uneven distribution of incoming solar energy. The importance of a sizeable heat source located *below* the atmosphere is one of the primary distinguishing characteristics of giant-planet atmospheric dynamics.

### 7.13 Uranus and Neptune

## Problems

7-1. *Effective Temperature.* Calculate the effective temperatures  $T_e$  for Mercury, Venus, Earth, Mars, and Jupiter, assuming the following albedos: 0.06, 0.78, 0.30, 0.17, and 0.45, respectively. For the terrestrial planets, compare their effective temperatures to their surface temperatures.

7-2. *The Greenhouse effect.* Modify the calculation (Section 7.2.2) of the radiative-equilibrium temperatures of a thin layer of gas that has infrared optical depth  $\tau$  and temperature  $T_{\text{gas}}$ , and is overlying a surface at temperature  $T_{\text{sur}}$ , to the case of two separate layers of gas, each with optical depth  $\tau/2$ . Assume as before that the gas and surface behave as black bodies. Assume that the gas layers radiate in the infrared. Plot  $T_{\text{gas1}}$ ,  $T_{\text{gas2}}$  and  $T_{\text{sur}}$  as a function of  $\tau$  and compare with the original case.

7-3. *Simple Climate Model with Ice-Albedo Feedback.* (A.P. Ingersoll)

When the Earth cools and the ice-cover increases, the albedo increases and the surface absorbs less sunlight. The following is a linear model that indicates under what conditions a positive feedback can lead to an ice-covered Earth. Let  $T(t)$  be the global mean surface temperature of Earth, and  $A(T, t)$  be the global mean albedo. Take the time-averaged albedo to be  $A_0 \approx 0.3$ . Let  $F(t)$  be the solar “constant,” which is currently  $F_0 = 1370 \text{ W m}^{-2}$ , and  $C$  be the column heat capacity:

$$C \approx C(\text{ocean}) \approx (4000 \text{ J kg}^{-1} \text{ K}^{-1})(10^3 \text{ kg m}^{-3})(2.5 \times 10^3 \text{ m}) = 10^{10} \text{ J m}^{-2} \text{ K}^{-1}. \quad (7.40)$$

Assume an emissivity  $\epsilon = 0.62$ , which is valid when the infrared flux is expressed in terms of the surface temperature. The governing equation is:

$$C \frac{\partial T}{\partial t} = \frac{F}{4}(1 - A(T)) - \epsilon \sigma T^4, \quad (7.41)$$

where  $\sigma = 5.67 \times 10^{-8} \text{ W m}^{-2} \text{ K}^{-4}$  is the Stefan-Boltzmann constant. Equation (7.41) is a nonlinear differential equation with dependent variable  $T(t)$ .

a) To linearize an equation we first need a basic-state solution. Determine the basic-state temperature,  $T_0$ , by setting  $F = F_0$  and recognizing  $\partial T_0/\partial t = 0$  in (7.41).

b) Assume that  $F = F_0$  and  $A = A_0$  in (7.41), and try the solution:

$$T(t) = T_0 + T'(t), \quad T' \ll T, \quad (7.42)$$

where  $T_0$  is the basic-state temperature and  $T'(t)$  is a small perturbation (the prime denotes a perturbation quantity, not a derivative). For small  $T'$  we can neglect nonlinear terms like  $(T')^2$ . Derive the linear equation:

$$\frac{\partial T'}{\partial t} + \frac{1}{\tau} T' = 0, \quad (7.43)$$

by keeping only constant terms and terms involving  $T'$ . Find the radiation time constant  $\tau$ .

c) Continue assuming  $A = A_0$  and  $T = T_0 + T'(t)$ , but now set:

$$F = F_0 + F'(t), \quad F' \ll F_0, \quad (7.44)$$

in (7.41). Derive the linear equation:

$$\frac{\partial T'}{\partial t} + \frac{1}{\tau} T' = \alpha \frac{T_0}{\tau} \frac{F'}{F_0}, \quad (7.45)$$

and find the coefficient  $\alpha$ . Find the solution to (7.45) by modeling the variation of the solar constant over geological time with a simple harmonic function:

$$\frac{F'}{F_0} = \gamma e^{i\omega t}, \quad (7.46)$$

where  $\gamma$  and  $\omega$  are constants, and it is understood that we want only the real part of (7.46) (leave it in complex form for convenience). Other functions for  $F'(t)$  can be constructed as linear combinations of terms of the form (7.46) by Fourier analysis.

d) Now, examine the fully perturbed system by setting:

$$\begin{aligned} T &= T_0 + T'(t), \\ F &= F_0 + F'(t), \\ A &= A(T_0) + \frac{dA}{dT}(T_0) T', \end{aligned} \quad (7.47)$$

in (7.41), where the expression for  $A$  is just a Taylor-series approximation. Derive the linear equation:

$$\frac{\partial T'}{\partial t} + \frac{1}{\tau} \beta T' = \alpha \frac{T_0}{\tau} \frac{F'}{F_0}, \quad (7.48)$$

and find the coefficient  $\beta$ . Find the solution when  $F'(t)$  is given by (7.46), and show that the sign of  $\beta$  controls whether the system is stable or unstable to small perturbations.

e) We estimate the function  $A(T)$  by using the following observations of the local albedo-temperature relationship on the present-day Earth:

latitude:	5°	15°	25°	35°	45°	55°	65°	75°	85°
T[K]:	299	299	294	288	281	274	266	258	250
A:	.22	.22	.25	.30	.35	.40	.50	.58	.65

Table 7.1

Assume that  $A = .20$  for  $T \geq 305$  K, and  $A = .70$  for  $T \leq 243$  K. The equilibrium flux normalized to the present-day flux,  $\hat{F}$ , is given by:

$$\hat{F}(T) = \frac{4\epsilon \sigma T^4}{F_0 (1 - A(T))}. \quad (7.50)$$

Plot  $T$  vs.  $\hat{F}(T)$ , and indicate the position of the present-day Earth. Show that  $\beta$  in (7.48) is related to the sign of  $dT/d\hat{F}$ . Indicate on the plot the stable region that is similar to the present-day Earth, the unstable region, and the stable, ice-covered region.

### References

- Atreya, S.K., J.B. Pollack & M.S. Matthews, 1989, *Origin and Evolution of Planetary and Satellite Atmospheres*, University of Arizona Press.
- Beatty, J.K. and A. Chaikin, 1999, *The New Solar System*, 4th ed., Sky Publishing.
- Gehrels, T. and M.S. Matthews, 1984, *Saturn*, University of Arizona Press.
- Gill, A., 1982, *Atmosphere-Ocean Dynamics*, Academic Press.
- Goody, R.M. & Y.L. Yung, 1989, *Atmospheric Radiation: Theoretical Basis*, 2nd ed., Oxford University Press.
- Houghton, J.T., 1986, *The Physics of Atmospheres*, 2nd ed., Cambridge University Press.
- Hunten, D.M., L. Colin, T.M. Donahue & V.I. Moroz, 1983, *Venus*, University of Arizona Press.